Annual AFOSR Astronautic Symposium, Denver, Colo. (April 1958).

[3] Rodriquez, E., "Method for determining steering programs for low thrust interplanetary vehicles," ARS J. 29, 783–788 (1959).

Shock-Wave Boundary-Layer Interaction on a Missile Nose Probe

M. D. Bennett*
Sandia Corporation, Albuquerque, N. Mex.

When a pressure probe is mounted on the nose of a missile, a compression corner is formed at the juncture of the probe base and vehicle nose. At supersonic speeds, the shock wave emanating from the compression corner interacts with the probe boundary layer to produce perturbations both downstream and upstream from the corner. To avoid flow interference at the pressure orifice, the afterbody of the probe must be sufficiently long that the orifice is located upstream of the shock-wave boundary-layer interaction region. Wind-tunnel tests were made to determine the critical length for a cone-cylinder probe at speeds from Mach 1.4 to 4.0 and freestream unit Reynolds numbers from 7.0×10^5 to 8.0×10^6/ft. In transitional flow with adiabatic wall temperature, the afterbody critical length is proportional to Mach number and angle of attack and inversely proportional to Reynolds number. In turbulent flow, the critical length is relatively small and apparently independent of Mach number, Reynolds number, and angle of attack.

Introduction

In some flight applications, a small probe is mounted on the nose of a missile to permit measurement of atmospheric properties such as pressure or density. At supersonic speeds, a shock wave emanates from the region where the probe joins the nose section of the vehicle. The abrupt increase in pressure through the shock wave results in a strong, adverse pressure gradient that can cause separation of the probe boundary layer. Consequently, the pressure distribution both downstream and upstream from the compression corner may be affected. If the extent of the shock-wave boundary-layer interaction in the upstream direction is sufficient to cause interference with flow at the probe orifice, measured pressure (or density) will be affected. In the extreme cases, the interference effect can amount to more than 50% of the true pressure. To eliminate flow interference, the afterbody of the probe may be made sufficiently long that the orifice is upstream of the interaction region.

Numerous studies of separated flow at supersonic speeds have been reported. The results indicate that any of the many variables that affect transition location can influence the extent of, and pressure distribution in, separated flow regions. Thus, in addition to the variables previously mentioned, surface roughness, stream turbulence, heat transfer, probe geometry, and vehicle nose geometry can affect the critical length of the probe afterbody.

Most of the previous studies have been concerned with the separated region in two-dimensional flows. The present study is concerned with the length of the separated flow ahead of a compression corner in an axially symmetric flow. Data at angles of attack up to 12° are presented.

Received January 29, 1963.

* Supervisor, Aerophysics Section.

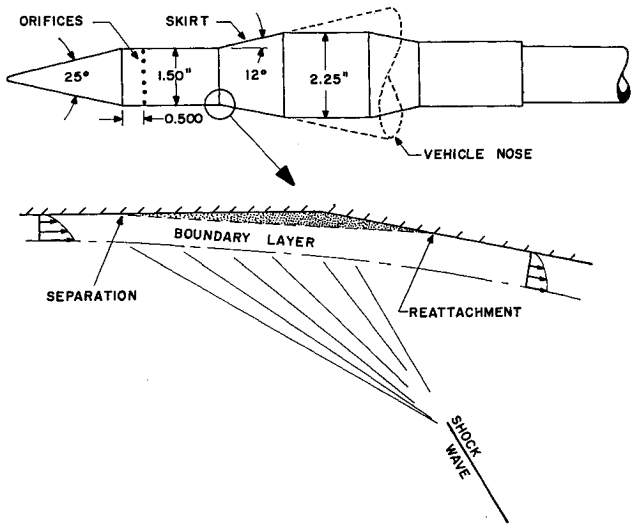

Fig. 1 Sketch of wind-tunnel model for shock-wave boundary-layer interaction tests.

Experiment

Tests were performed in a 12- × 12-in. wind tunnel at speeds from Mach 1.4 to Mach 4.0; freestream Reynolds number (V_0/ν_0) range was approximately 7.0×10^5 to 8.0×10^6/ft. The geometry of the pressure probe and an exaggerated sketch of the shock-wave boundary-layer interaction are shown in Fig. 1. The model was supported by a swept strut attached to the side wall of the tunnel. The leading edge of the strut was located about 2.5 in. downstream of the broken section shown at the right-hand margin in Fig. 1. The probe was fixed with respect to the tunnel, and the axial position of the skirt (the forward section of which represents the tip of the vehicle nose) was remotely controlled. The diameter of the skirt was made sufficiently large that the reattachment point was located on the forward section of the skirt; the reattachment point was determined from schlieren photographs and spark shadowgraphs. Clearance between the skirt lip and the cylindrical section of the probe was about 0.004 in. There were 24 $\frac{1}{16}$-in.-diam orifices located $\frac{1}{2}$ in. downstream from the cone-cylinder shoulder and equally spaced around the periphery of the probe. The orifices were manifolded in a tube located on the axis of the

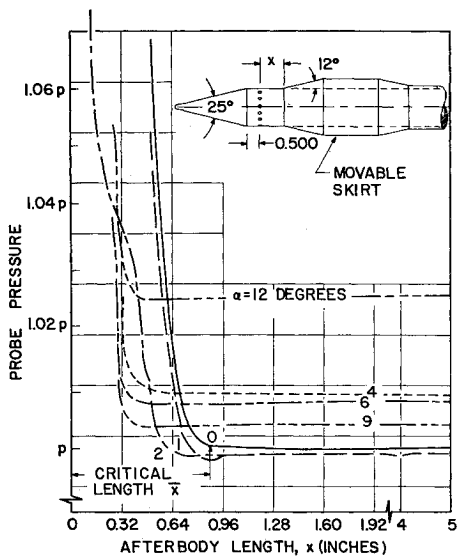

Fig. 2 Effect of skirt position on probe pressure at Mach 1.4 ($V_0/\nu_0 = 0.58 \times 10^6$/in.).

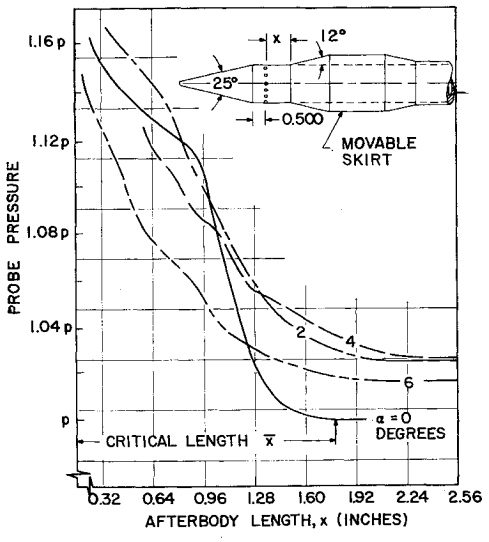

Fig. 3 Effect of skirt position on probe pressure at Mach 1.4 ($V_0/\nu_0 = 0.13 \times 10^6$/in.).

probe, and the manifolded pressure was measured by means of a pressure transducer. The transducer and a potentiometer that indicated skirt position were used in conjunction with an X-Y plotter to provide a continuous trace of the shock-wave boundary-layer interaction effect. Generally, at the beginning of each test, the skirt was in the downstream position (5 in. from the skirt leading edge to the probe orifices). During the tests, the skirt was moved forward toward the probe orifices and then returned to the original position. There was no apparent aerodynamic hysteresis.

To locate the position of boundary-layer transition, the Azobenzene technique was used. Azobenzene sublimates rapidly in turbulent flow and is relatively unaffected in laminar flow. Two tests were made at Mach 1.4 with the skirt removed. The transition position was located 0.3 ± 0.1 in. downstream of the orifices when $V_0/\nu_0 = 6.36 \times 10^6$/ft, and 1.8 ± 0.2 in. downstream of the orifices when $V_0/\nu_0 = 4.20 \times 10^6$/ft.

Reference 1 shows that the principal variable controlling pressure distribution in two-dimensional, separated flows is the location of transition relative to the separation and reattachment positions. The classification of separated flows is divided into three regimes: "pure laminar" when transition is downstream of the reattachment position, "transitional" when transition is between the separation and reattachment

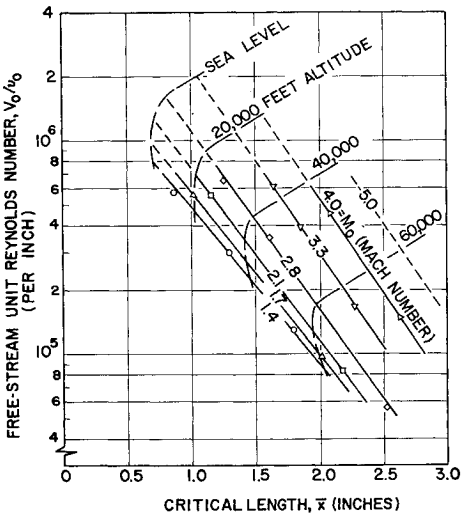

Fig. 4 Afterbody critical length at 0° angle of attack as a function of freestream Reynolds number (transitional separation).

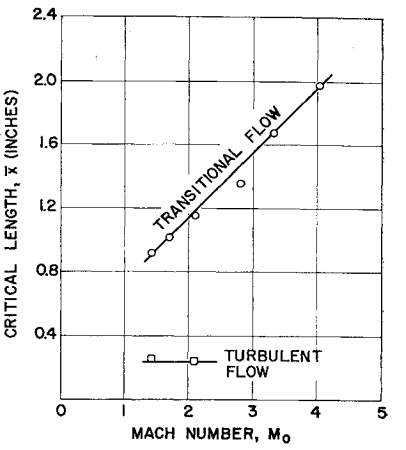

Fig. 5 Afterbody critical length at 0° angle of attack as a function of Mach number for transitional and turbulent separation ($V_0/\nu_0 = 0.57 \times 10^6$/in.).

positions, and "turbulent" when transition is upstream of the separation position. Using this classification, the flow is normally transitional for the results reported here. Additional data are presented with a turbulent boundary layer that was generated by a trip.

Results

Figure 2 shows a typical record of the effect of skirt position x on probe pressure p for several constant angles of attack α. The freestream Mach and freestream unit Reynolds numbers are $M_0 = 1.4$ and $V_0/\nu_0 = 6.96 \times 10^6$/ft, respectively. At each angle of attack there is a critical distance aft of the orifices beyond which the skirt position does not affect probe pressure. When the skirt position is less than the critical length, the pressure is increased. The extent of the increase is proportional to the change in position. The critical length of the probe afterbody, designated $\bar{x}$ at $\alpha = 0°$, is largest at small angles of attack.

The interaction effect at a relatively small Reynolds number ($V_0/\nu_0 = 1.56 \times 10^6$/ft) and $M_0 = 1.4$ is shown in Fig. 3. At the smaller Reynolds number, critical length $\bar{x}$ is relatively large, and the larger angles of attack dictate greater critical lengths. Data at angles of attack larger than 6° were not obtained under these particular test conditions because of model-tunnel flow blockage.

Figure 4 shows the accumulation of all transitional-flow data at 0° angle of attack. It was found that the data could be represented by straight lines on a semilog graph. The results have been extrapolated to Mach 5, and lines corresponding to constant flight altitude are indicated. Critical length increases with increasing Mach number and decreasing Reynolds number. A recent investigation of flow separation on cone-cylinder-flare configurations at Mach 5 is presented in Ref. 2. Although a direct comparison of the data cannot be made with the results presented in Fig. 4, the data are in qualitative agreement.

The angle-of-attack data of the present study may be summarized as follows. For angles of attack up to 12°, the maximum critical length, and also the maximum value of the ratio of critical length at $\alpha \pm 0$ to critical length at $\alpha = 0$, occurred at the condition where $M_0 = 2.1$, $\alpha = 9°$, and $V_0/\nu_0 = 0.99 \times 10^6$/ft. The maximum value of the critical length was $2.15\bar{x}$, or approximately 4.60 in.

Figure 5 shows a comparison of afterbody critical length at 0° angle of attack in turbulent and transitional flows with constant Reynolds number ($V_0/\nu_0 = 6.84 \times 10^6$/ft). The critical length in transitional flow is several times the value in turbulent flow. In turbulent flow, the critical length is practically independent of angle of attack for angles up to at least 12°. The turbulent boundary layer was generated with a $\frac{3}{8}$-in.-wide coating of commercial number 180 carborundum grit around the conical nose surface of the probe. The carborundum coating was located $\frac{1}{2}$ in. upstream of the cone cylinder shoulder.

Conclusions

The critical length of the afterbody of a cone-cylinder probe on a slender nosed (12° half angle) vehicle has been investigated experimentally at Mach numbers from 1.4 to 4.0 and angles of attack up to 12°. In transitional flow with adiabatic wall temperature and at freestream Reynolds numbers from 7.0×10^5 to 8.0×10^6/ft, the critical length increases with increasing Mach number and angle of attack and decreases with increasing Reynolds number. In turbulent flow, the critical length is relatively small and apparently independent of Mach number, Reynolds number, and angle of attack.

References

[1] Chapman, D. R., Juehn, D. M., and Larson, H. K., "Investigation of separated flows in supersonic and subsonic streams with emphasis on the effect of transition," Natl. Advisory Committee for Aeronaut. TN 3869 (March 1957).

[2] Schaefer, J. W. and Ferguson, H., "Investigation of separation and associated heat transfer and pressure distribution on cone-cylinder-flare configurations at Mach five," ARS J. **32**, 762–770 (1962).

Measurement of Mean Particle Size in a Gas-Particle Flow

R. A. Dobbins*

Brown University, Providence, R. I.

Nomenclature

c_n	=	particle number concentration
D	=	particle diameter
D_∞	=	maximum particle size present
F/F_0	=	optical transmission
$K(D,m)$	=	extinction coefficient or scattering coefficient for dielectric particles
l	=	optical path length
m	=	refractive index of particle relative to surrounding medium
$N_r(D)$	=	particle size distribution function

THE use of metallic additives in solid propellants results in the formation of particulate products of combustion, the sizes of which influence the performance of the rocket motor. Losses resulting in reduced thrust will occur if the particle size is not small enough to assure thermal and dynamic equilibrium between particulate and gaseous phases The importance of techniques of measuring particle size therefore is apparent. Probably the most accurate method of measuring particle size distribution is to obtain a representative sample for observation by appropriate methods of microscopy. The work reported by Sehgal[1] appears to be an excellent example of the application of this type of technique. Although the most accurate means of measurement is preferred on many occasions, it is natural to inquire as to whether other techniques are available which possess advantages of greater convenience or more universal applicability. The scattering properties of the particles appear to provide a basis for a technique that fulfills this description.

Received March 15, 1963. This work was sponsored by the Hercules Powder Company, Allegany Ballistics Laboratory, under Contract NOrd 16640. The author wishes to express his gratitude to D. J. Carlson of the Aeronutronic Division of Ford Motor Company for supplying the detailed experimental data.

* Assistant Professor of Engineering. Member AIAA.

The advantages of a technique based on scattering properties are, as noted by van de Hulst,[2] the rapidity of the evaluation and its applicability when the particles are inaccessible, i.e., when they cannot be sampled properly. A starting point for an investigation on the use of scattering properties in the simplest possible manner is afforded by considering the optical transmission of the gas-particle fluid.

The transmission law applicable for a polydispersion of spherical particles is

$$\frac{F}{F_0} = \exp\left[-\frac{\pi}{4} c_n l \int_0^{D_\infty} K(D,m) N_r(D) D^2 dD \right] \tag{1}$$

The particle size distribution function $N_r(D)$ is defined such that

$$\int_{D_1}^{D_2} N_r(D) dD = P[D_1 < D < D_2] \tag{2}$$

where $P[D_1 < D < D_2]$ represents the relative probability of occurrence of particles larger than D_1 and smaller than D_2. The extinction coefficient is determined from electromagnetic theory as described by van de Hulst.[2]

The transmission law can be written in a more useful form by introducing certain integrated quantities. The mean extinction coefficient $\bar{K}$ and the volume-to-surface mean diameter are defined as

$$\bar{K} \equiv \frac{\int_0^{D_\infty} K(D,m) N_r(D) D^2 dD}{\int_0^{D_\infty} N_r(D) D^2 dD} \tag{3}$$

$$D_{32} = \frac{\int_0^{D_\infty} N_r(D) D^3 dD}{\int_0^{D_\infty} N_r(D) D^2 dD} \tag{4}$$

and the particle volume concentration c_v is introduced:

$$c_v = \frac{\pi}{6} c_n \int_0^{D_\infty} N_r(D) D^3 dD \tag{5}$$

The transmission law now can be expressed as

$$\frac{F}{F_0} = \exp\left(-\frac{3}{2} \frac{\bar{K} c_v l}{D_{32}} \right) \tag{6}$$

Although the determination of a complete distribution function from an optical transmission test generally is not possible, Eq. (6) suggests that a determination of the mean diameter represented by D_{32} may be feasible.

For the purpose of exploring this possibility, the mean scattering coefficient $\bar{K}$ was calculated over a wide range of D_{32} initially for rectangular and parabolic distributions of dielectric particles, the refractive index of which is near unity, $(m - 1) \ll 1$. The results show that the largest discrepancy between the mean scattering coefficients yielded by these two radically different distribution functions for given D_{32} was only 3% and that usually the two coefficients were more nearly coincident. The mean scattering coefficient for skewed distribution functions possessing a finite maximum diameter D_∞ now is being investigated. The results obtained thus far indicate that the $\bar{K}$ for these functions, which are empirically representative of particle size distributions, is very close to that of the parabolic distribution possessing the same value of D_{32}. A study of mean scattering coefficient for polydispersions of dielectric particles of finite $(m - 1)$ is now in progress. The presently available results indicate that the $\bar{K}$ is primarily a function of D_{32} independent of the shape of the distribution function, or, in alternate form,

$$D_{32} = f(\bar{K}/D_{32}) \tag{7}$$

Figure 1 may be regarded as expressing this functional relationship in appropriate nondimensional form for parabolic and rectangular distribution functions of particles of small $(m - 1)$. Thus, an optical transmission test on a gas-